MEDWIN PUBLISHERS
Committed to create value for Researchers

Medicinal & Analytical Chemistry International Journal
ISSN: 2639-2534

Electrochemical Oxidation of Catechol in the Presence of Methimazole: Application of Square-Wave Voltammetric Detection of Methimazole to Pharmaceutical Formulations

Torriero AAJ*

School of Life and Environmental Sciences, Deakin University, Australia

***Corresponding author:** Angel A J Torriero, School of Life and Environmental Sciences, Deakin University, Burwood, Victoria 3125, Australia, Tel: +61392446897; Email: angel.torriero@deakin.edu.au

Research Article

Volume 3 Issue 2

Received Date: June 10, 2019

Published Date: June 24, 2019

DOI: 10.23880/macij-16000139

Abstract

The electrochemical oxidation of catechol has been studied in 0.1 M phosphate (pH 7.0) buffered aqueous solutions in the presence of methimazole as a nucleophile. Cyclic voltammetric and controlled-potential coulometric data demonstrate the occurrence of nucleophilic addition to the electrochemically-generated benzoquinone molecule following a 1-4 addition mechanism. The resulting ring-substituted product is more easily oxidized than the original catechol, leading to an increase in the anodic current, which is proportional to the concentration of methimazole. The second-order rate constant for the homogeneous reaction between the electrochemically-generated o-quinone and methimazole was estimated by comparison of digital simulations of the cyclic voltammograms and experimental data. Square-wave voltammetry was applied to provide a very sensitive voltammetric determination of methimazole with a linear peak current response over the concentration range of 0.03 to 40μM, with a detection limit of 12nM. The presence of excipients commonly found in pharmaceutical preparations produced no appreciable change to the voltammetric response of Methimazole.

Keywords: Methimazole; Catechol; Glassy Carbon; Cyclic Voltammetry; Square-Wave Voltammetry

Abbreviations: MWCNT: Multi-Walled Carbon Nanotube, GC: Glassy Carbon, OSWV: Osteryoung Square-Wave Voltammetry.

Introduction

Methimazole (1-methyl-2-mercaptoimidazole), MMI, is a thiourea derivative which has been reported to be an inhibitor of mushroom tyrosinase and dopamine β-hydroxylase enzymes [1,2]. MMI also inhibits iodine and peroxidase from their normal interactions with thyroglobulin to form thyroxine and triiodothyronine (two thyroid hormones) [3]. Although it is not available in every country, MMI is used as a drug to manage hyperthyroidism associated with Grave's disease, but it has side effects such as nephritis, liver cirrhosis, irritation of the skin, allergies, pharyngitis with fever and possible decrease of white blood cell concentration in the blood [4]. An alternative oral drug that has been used is carbimazole, which is converted after absorption to the

active drug MMI. This prodrug produces less frequent gastrointestinal problems with respect to MMI.

According to Anderson [5] some thiol compounds act as inhibitors of tyrosinase because of their ability to reduce o-quinones functionalities back to the parent o-dihydroxyphenols (e.g. thioglycollate and mercapto benzothiazole at certain concentrations) [6,7] while other thiol compounds act as inhibitors because of their ability to form a stable conjugate with the o-quinones molecules (GSH, cysteine, methionine, etc.) [8]. Since methimazole is a thiol compound, it is important to find out its potential ability to reduce and/or to conjugate with electrochemically generated o-quinone molecules.

The identification and quantification of MMI are of great importance within the clinical chemistry, pharmaceutical formulations and quality control areas [9]. Analytical techniques available for the determination of MMI include thin layer chromatography, high-performance liquid chromatography with ultraviolet detection [10] spectroscopy, [11-13] capillary zone electrophoresis [14] and chemiluminescence (table 1) [15]. Electroanalytical methods have also been very successful for the determination of thiol in pharmaceutical and clinical preparations [16]. Results in Table 1 reveal that chemically modified electrodes present a wide linear range and low detection limit. However, they are generally sophisticated and relatively expensive devices. Some of the postulated sensor systems are certainly not a new technology, as they were widely used to identify and quantify other thiol-based molecules [17-19]. In addition, the use of nanomaterials, such as carbon nanotubes, is normally justified by an increase in the electroactive surface area of the electrode, which generally results in an improvement in the electrode sensitivity. However, as possible to be seen from Table 1, the obtained detection limits with and without multi-walled carbon nanotube materials are significantly similar.

Detection method	Matrix	Linear range	Detection limit	Ref.
HPLC-UV	Pl	5.8 – 70 µM	1.8 µM	10
Flow-injection spectrometry	Ph-Pl	10 - 500 µM	3 µM	11
Capillary-zone electrophoresis	Ph-Se	1 – 500 µM	0.8 µM	14
Chemiluminescence	Ph	17.5 – 876 µM	0.9 µM	15
Potentiometric titration	Ph	1 – 700 µM	0.5 µM	9
OSWV- fluorine-doped tin oxide electrodes	Ph	6 – 240 µM	1.98 µM	20
CA - Screen-printed enzymatic biosensor	Ph	0.074–63.5 µM	56 nM	21
CA - rutin/ /MWCNTs/GCE	Ph-Se	0.1 – 26 µM	18 nM	22
CA - oxovanadium(IV) Schiff-base complex/CPE	Ph	0.9 – 100 µM	0.8 µM	23
DPV – MWCNTs-Salen-Co(III)-MIP electrode	Ph-Ur	4.0 – 50 µM	0.4 µM	24

Pl: plasma; Ph: pharmaceutical; Se: serum; Ur: urine; MWCNT: multi-walled carbon nanotube; GCE: glassy carbon electrode; CPE: carbon paste electrode; DPV: differential pulse voltammetry; CA: chronoamperometry.
Table 1: A comparison of methods available for the determination of methimazole.

Chemically modified electrodes based on transition metal complex have been widely used for the electrocatalytic detection of thiols [25-28]. Poor selectivity using modified electrodes and the very weak voltammetric response of the target analyte at bare electrodes are often serious problems in detection of thiols. A number of strategies for improving the electrode response have been investigated. Typically, they are based on the application of reversible redox indicators such as hydroquinones and catechols and rely upon the electrochemical oxidation of the indicator species to the corresponding quinoid intermediate [29,30]. Although 1,4-benzoquinone derivatives have been even more extensively studied because they are easier to prepare with higher yields [31], Nematollahi et al. has shown that 1,2-hydroquinone (catechol) derivatives can be oxidized electrochemically to 1,2-benzoquinone, which are quite reactive and can readily react with a variety of nucleophiles [32-34].

In this paper, the mechanism associated with the electrochemical oxidation of catechol at a glassy carbon (GC) electrode in the absence and presence of MMI is discussed. In addition, the electrochemically-initiated reaction of MMI with catechol is used to provide a simple and cost-effective electroanalytical signal, which can be correlated to the thiol concentration.

Materials and methods

Methimazole (MMI, 99%), catechol (99%), caffeic acid (98%), 1,4-hydroquinone (99.5%) and 4-tert-butylcatechol (99%) were purchased from Sigma-Aldrich and used as received without further purification. Aqueous solutions were prepared using Milli-Q water (Millipore, USA) system. Synthetic tablet samples were prepared by spiking a placebo (a mixture of tablet excipients) with an accurately calculated amount of MMI. Then, they were ground to a fine powder and dissolved and diluted to the desired volume with aqueous 0.1 M phosphate (pH 7.0) buffer solution. The pH of these buffer solutions was monitored with a pH meter (Thermo Scientific Orion Dual Star, Australia) and adjusted to pH 8 using either HCl or NaOH.

Electrochemical experiments were performed in unstirred solutions using a Gamry Interface1000 potentiostat (Gamry, USA), using a positive feedback routine to compensate for the ohmic resistance. Cyclic voltammograms were obtained at scan rates (v) in the range 0.030-0.80 V s^{-1}, using a conventional three electrode arrangement, consisting in a 3.0 mm diameter GC working electrode (ALS, Japan), a platinum wire as a counter electrode and an Ag|AgCl|3 M NaCl reference electrode (ALS, Japan). Prior to each experiment, the working electrode was polished with 0.3μm alumina (Buehler, Lake Bluff, IL) on a clean polishing cloth (Buehler), sequentially rinsed with distilled water and acetone, and then dried with lint-free tissue paper. The GC effective area (A = 0.070 cm^2) was determined from cyclic voltammograms using the peak current derived as a function of the square root of scan rate from the oxidation of a 1.0mM solution of ferrocene in CH_3CN (0.1 M Bu_4NPF_6 as the supporting electrolyte; ferrocene diffusion coefficient = 2.3 $\times 10^{-5}$ cm^2 s^{-1}) degassed with N_2 and application of the Randles–Sevcik relationship [35].

Controlled potential bulk electrolysis was performed using a glassy carbon tube working electrode and a platinum-gauze auxiliary electrode separated from the test solution by a fine-porosity glass frit. All voltammetric experiments were carried out at ambient temperature (21 ± 1°C). The commercially available software package DigiElch was used to simulate the voltammetric responses.

Results and Discussion

Initial electrochemical studies to determine the mechanism of the reaction between catechol and MMI were carried out using cyclic voltammetry. Figure 1A, curve a, shows a typical cyclic voltammetric response of catechol in buffered solution (pH 7.0), at a scan rate of 0.1 Vs^{-1}. The cyclic voltammogram has the characteristics of a quasi-reversible two-electrons two-protons reaction mechanism (Eq 1) showing well-separated anodic (peak I_a, E_{pa}= 0.31 V) and cathodic peaks (peak I_c, E_{pc}= 0.06 V). The voltammetric profile does not change significantly even after 20 cycles of potential. The peak current ratio I_{pc}/I_{pa} (where I_{pa} = anodic peak current and I_{pc} = cathodic peak current) is close to unity, particularly after repetitive recycling of potential, which represents a criterion for the stability of the o-benzoquinone product produced at the electrode surface. It is noteworthy that the hydroxylation or dimerization reactions are too slow to be observed on the cyclic voltammetry time scale [36].

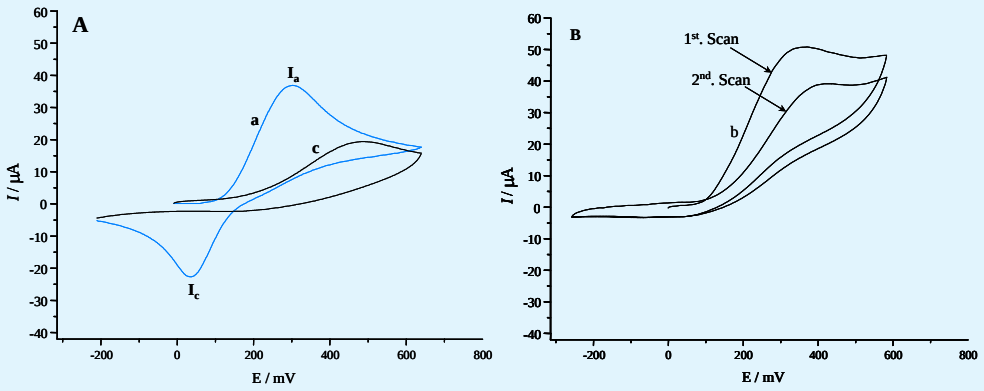

Figure 1: Cyclic voltammogram of **(A)** 1.0mM catechol (a), 1.0mM methimazole (c) and **(B)** first and second cycles of 1.0mM catechol in the presence of 1.0mM methimazole (b) at a glassy carbon electrode (3.0 mm diameter) in 0.1 M phosphate buffer (pH 7.0). Scan rate 0.1 Vs^{-1}.

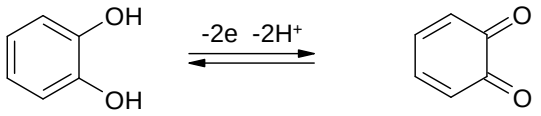

(1)

The voltammetric oxidation of catechol to the corresponding quinone in the presence of MMI was also studied. Figure 1B, curve b provides an example of the voltammograms observed upon addition of 1mM MMI. This voltammogram shows a clear loss of reversibility with an enhancement of the anodic peak current. Given that the irreversible peak potentials for the direct oxidation of MMI at the GC electrode surface are 0.19 V more anodic with respect to oxidation of catechol (Figure 1A, curve c), the increase in the anodic current on voltammogram b is attributed to the regeneration of catechol resulting from the reaction of o-benzoquinone with MMI (Eqs 2 and 3). Consequently, the detected current, I (eq 4), is the sum of two contributions:

- The diffusion-controlled current (I_d) of catechol in the absence of MMI.
- The current ($I_{catechol\text{-}MMI}$) associated to the oxidation of the resulting adduct product (Eq 3).

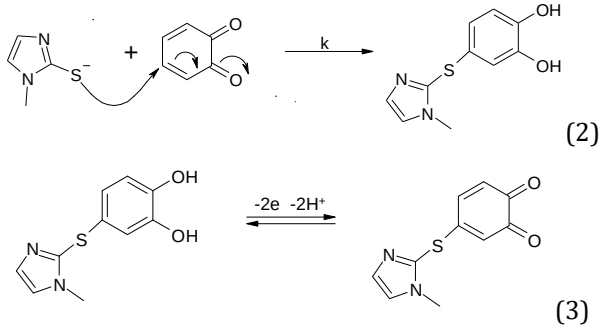

(2)

(3)

$$I = I_d + I_{catechol\text{-}MMI} \quad (4)$$

The cyclic voltammogram for the direct oxidation of MMI on a GC electrode in phosphate buffered solution (pH 7.0) depicted in Figure 1A, curve c shows an oxidation peak at around 0.49 V vs Ag|AgCl|3 M NaCl when the potential is scanned in the anodic direction. When the potential scan direction is reversed, no complementary reduction peak is observed over the scan rate range studied (0.03-0.8 V s^{-1}). This behavior is typical for a fast irreversible chemical reaction coupled to the charge-transfer step. The direct electrochemical oxidation of MMI has been demonstrated to proceed via a two-electron irreversible oxidation process [20].

Figure 2A provides examples of cyclic voltammetric responses for 1mM catechol obtained in the absence and presence of increasing concentrations of MMI. The addition of MMI triggers a considerable increase in the anodic peak current. This behavior and the loss of the corresponding cathodic peak are consistent with the mechanism proposed in Eqs 1-3.

Figure 2B shows the effect of scan rate on the oxidation of 1mM catechol in the presence of 1mM MMI. As the scan rate decreases, the peak current ratio I_{pc}/I_{pa} becomes < 1 and the cathodic peak I_c disappears. The oxidation peak current (I_{pa}) shows a linear dependence on $v^{1/2}$, revealing that the electrochemical oxidation of catechol in the presence of MMI remains a diffusion-controlled process under these experimental conditions. As expected, at large scan rates the voltammetric behavior resembles that of catechol in the absence of MMI. At the same time, a new oxidation peak appears at 0.52 V vs Ag|AgCl|3 M NaCl (see voltammogram g in Figure 2 B), which corresponds to the direct oxidation of MMI at the GC working electrode.

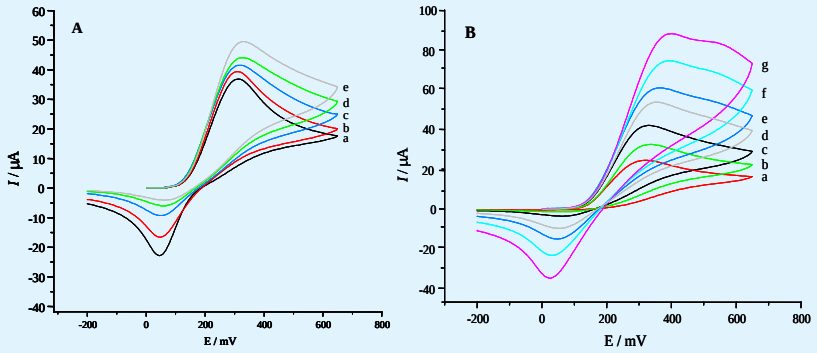

Figure 2: Cyclic voltammograms of 1.0mM catechol in 0.1 M phosphate buffer (pH 7.0) at a GC electrode (3.0 mm diameter) **(A)** as a function of MMI concentration; c_{MMI}: (a) 0.0, (b) 0.22, (c) 0.48, (d) 0.71, (e) 1.0mM; at a scan rate of 0.1 Vs^{-1}. **(B)** Cyclic voltammograms of 1.0mM catechol in the presence of 1.0mM MMI as a function of scan rate; v = (a) 0.03, (b) 0.06, (c) 0.1, (d) 0.2, (e) 0.3, (f) 0.5, and (g) 0.8 Vs^{-1}.

The influence of acidity on peak current was assessed in buffered solutions over the pH range of 4 to 8 (data not shown). The I_{pc} obtained in a 1mM catechol solution containing 1mM MMI was found to increase steadily as the acidity of the solution was increased. This can be attributed to the fact that as the pH of the solution is lowered, the thiol functionality of MMI will be increasingly protonated (pKa ~ 8.0), hence the nucleophilic character of the thiol moiety diminished. Increasing the pH, therefore, optimise the magnitude of the response, but an operational limit is reached since in alkaline solutions the nucleophilic hydroxyl ions compete with thiol. Consequently, a pH value of 7.0 (0.1 M phosphate buffer) was chosen for analytical applications.

Controlled-potential bulk electrolysis at the potential of 0.39 V vs. Ag|AgCl|3 M NaCl was performed in an aqueous solution of 0.1 M phosphate buffer (pH 7.0) containing 2 mmol of catechol and 2 mmol of MMI. The electrolysis was terminated when the current decrease by more than 95% of its initial value. During the course of the electrolysis, anodic peak I_a decreases and disappears when the charge consumption reaches 4.25 electrons per molecule of catechol. This result is consistent with the ECE (electron transfer-chemical reaction-electron transfer) mechanism proposed for the electrochemical oxidation of catechol in the presence of MMI (Eqs 1-3).

The second-order rate constants k_f, for the homogeneous rate constant between the catechol and MMI was estimated by comparison of digital simulations of the cyclic voltammograms and experimental data (Figure 3A). Simulations based on the mechanism outlined in Eqs 1-3 give excellent agreement with experimental observations made over a wide range of catechol (0.2-10mM) and MMI concentrations (0.02-10mM), when the rate constant of 5 x 10^5 M^{-1} s^{-1} is employed. Determinations of the rate constants were also performed at different scan rates (from 0.03 to 0.8 V s^{-1}) to minimize the interference of natural convection in the electrochemical response, which is normally observed at scan rates ≤0.05 V s^{-1}.

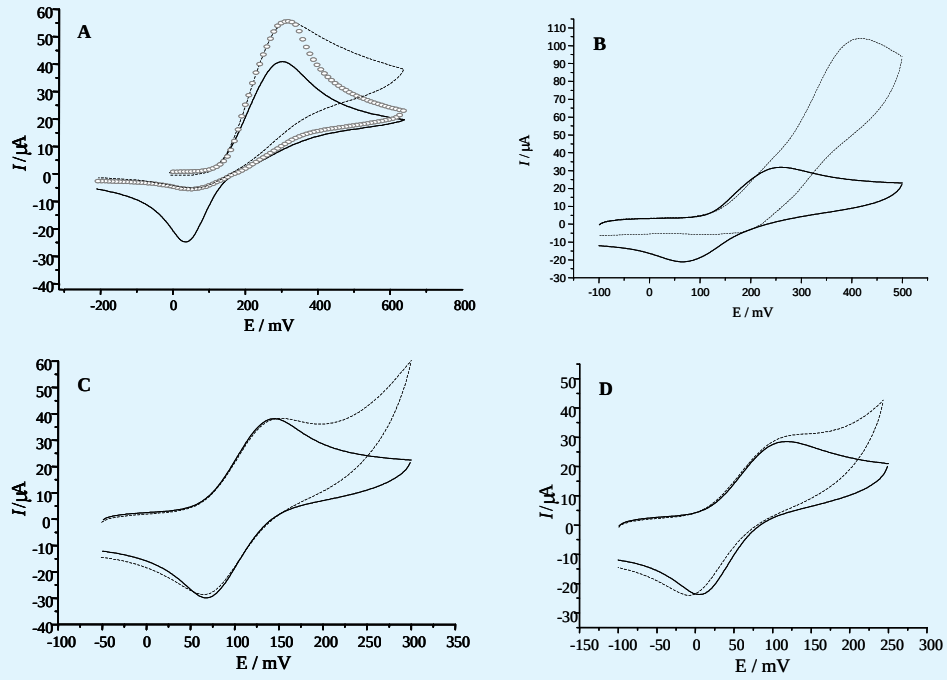

Figure 3: Cyclic voltammograms of (A) 1.0mM catechol, (B) 1.0mM caffeic acid, (C) 1.0mM 1,4-hydroquinone and (D) 1.0mM 4-tert-butylcatechol in the absence (–) and in the presence of methimazole (---) in 0.1 M phosphate buffer (pH 7.0). (○) Simulated cyclic voltammogram using DigiElch simulation software. Working electrode: glassy carbon (3.0 mm diameter), scan rate: 0.1 Vs^{-1}. Simulation parameters: T = 294 K, electrode area = 0.070 cm^2, charge-transfer coefficient (α) = 0.5, heterogeneous standard rate constant (k_s-catechol) = 0.001 cm s^{-1}, k_s catechol-MMI product = 0.001 cm s^{-1}, equilibrium constant (K_{eq}) = 3 × 10^4. $E^{\circ}_{catechol}$= 0.15 V, $E^{\circ}_{catechol\text{-}MMI\ product}$ = -0.3 V, Diffusion coeficient of catechol ($D_{catechol}$) = 7.6 × 10^{-6} cm^2 s^{-1}, The D_{MMI} and products were arbitrarily set to 1 × 10^{-5} and 7.6 × 10^{-6} cm^2 s^{-1}, respectively.

From the results of controlled-potential electrolysis with voltammetric monitoring and digital simulation, it is possible to hypothesize that the electrochemical oxidation of catechol (Eq 1) triggers the reaction sequence shown in Eqs 2 and 3. In this mechanism, MMI attacks the o-benzoquinone electrochemically generated in para-position respect to one of the oxygen atoms via nucleophilic addition (1-4 addition) reaction to form a reduced addition product (Eq 2). This product, which catechol ring is further activated by the new moiety, is subsequently oxidised in a further two-electron transfer process. Hence, the enhanced oxidation current is attributed to the oxidation of MMI-catechol adduct that arises through the electrochemically initiated reaction. Given that the direct oxidation of MMI at the electrode occurs at a more positive potential (Figure 1A, curve c) the increase in the magnitude of catechol oxidation peak can solely be attributed to the oxidation of the adduct, which redox potential should be more cathodic respect to the catechol redox potential.

The electrochemical response is expected to depend on the chemical nature of the catechol derivative. However, provided the catechol derivatives retain the capacity for electrochemical conversion to a quinone intermediate, they are expected to react with MMI. To this end, three different derivatives of catechol were examined: caffeic acid, 1,4-hydroquinone and 4-tert-butylcatechol. Voltammograms obtained in the absence and presence of 1.0mM of MMI are shown in Figure 3. From this figure, it is possible to see that the homogeneous reaction between MMI and the benzoquinone derivatives from 1,4-hydroquinone and 4-tert-butylcatechol are considerably slow to be observed on the cyclic voltammetry time-scale. This may be a consequence of the steric effect of the hydroxyl and tert-butyl moieties. Clearly, both catechol and caffeic acid react with MMI. However, the anodic peak potential for the caffeic acid-MMI adduct is more positive respect to catechol and in the same potential area where the direct oxidation of MMI occurs. Consequently, catechol was selected for the analytical determination of MMI.

The applicability of the previously described electrochemical reaction between catechol and MMI to the identification and quantification of MMI in different samples was examined using Osteryoung square-wave voltammetry (OSWV). Figure 4 illustrates the OSWV for 1mM catechol at pH 7.0 in the absence and presence of MMI (voltage step: 20 mV; pulse amplitude: 25 mV and frequency: 15 Hz). Clearly, the addition of MMI to the catechol solution gives an increase in the anodic peak current. A linear relationship (ΔI (μA) = 0.05 + 0.23 c_{MMI}) was observed between ΔI and the MMI concentration over the range of 0.03 and 40 μM (R^2 = 0.999); with a detection limit of 12nM (S/N = 3). Where ΔI is the increase in the oxidation current from catechol associated with the addition of MMI. Repetitive measured on standard solutions (n = 8) containing 1.0mM of catechol and 20μM of MMI gave a percentage standard error of ≤ 4.0%. No interferences were encountered on the addition of common tablet excipients, such as lactose, magnesium stearate, hydroxymethyl propyl cellulose, titanium oxide, polyethylene glycol. Therefore, it may be concluded that the excipients may not interfere with the determination of MMI in commercial tablet samples (Table 2). Precision and Recovery studies were performed by adding a known amount of MMI to a synthetic mixture. The recovery was 99.93 ± 0.16 % (Table 3) and the precision was 5.05 % within the range 5.0-20mg.

Sample No	Pure MMI sample (20.0 mM)	Synthetic MMI tablet sample (n = 5) (mM)
1	20.15	20.1
2	19.77	19.8
3	20.12	20.12
4	19.89	19.85
5	20.21	20.2
6	19.8	19.85
X	19.99 ± 0.08	19.98 ± 0.07
SD	0.19	0.17
CV (%)	0.95	0.85

[a]X (mM), mean ± S.E., standard error; SD, standard deviation; CV, coefficient of variation.

Table 2: Determination of methimazole in the presence and absence of tablet excipients by the OSWV method.

Added (MMI) (mg)	Found (mg) ± SD[a]	Recovery (%)	CV[b] (%)
5	4.99 ± 0.05	99.8	0.1
10	10.03 ± 0.09	100.03	0.9
15	14.97 ± 0.19	99.8	1.3
20	20.02 ± 0.28	100.1	1.4

SD[a], standard deviation; CV[b], coefficient of variation.

Table 3: Accuracy and precision data for the determination of methimazole by the OSWV method.

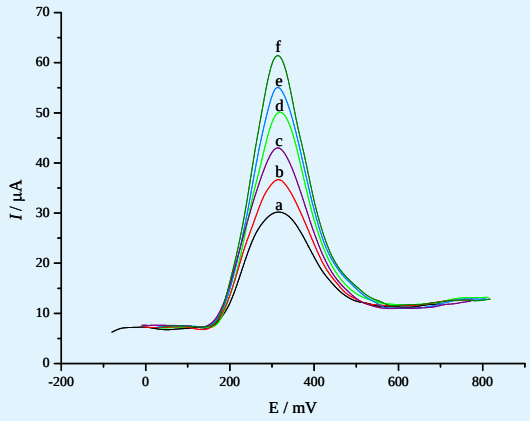

Figure 4: Square-wave voltammograms of 1.0mM catechol in 0.1 M phosphate buffer (pH 7.0) in the absence and presence of MMI; c_{MMI}: (a) 0.0, (b) 0.05, (c) 0.1, (d) 0.15, (e) 0.2, (f) 0.25 μM. Working electrode: glassy carbon (3.0 mm diameter), voltage step: 20 mV; pulse amplitude: 25 mV and frequency: 15 Hz.

Conclusion

Catehol was electrochemically oxidised to o-benzoquinone, which homogeneously react with MMI to form a catechol-MMI adduct. This reaction follows an ECE mechanism, with a total of 4 electrons being transferred. The kinetics for the reaction of the electrochemically generated two-electron oxidation product of catechol with MMI was estimated by comparison of digital simulations of the cyclic voltammograms and experimental data. Simulations based on the mechanism outlined in Eqs 1-3 give excellent agreement with experimental observations made over a wide range of catechol (0.2-10mM) and MMI concentrations (0.02-10mM). The use of the OSWV method provides a simple and selective method for the determination of MMI in pharmaceutical formulations. Because excipients do not interfere significantly with the electrochemical response, the proposed analytical technique is more simple, sensitive, accurate and precise than other previously reported techniques.

References

1. Hanlon DP, Shuman S (1975) Copper ion binding and enzyme inhibitory properties of the antithyroid drug methimazole. Experientia 31(9): 1005-1006.

2. Stolk JM, Hanlon DP (1973) Inhibition of brain dopamine-β-hydroxylase activity by methimazole. Life Sciences 12(9): 417-423.

3. Aletrari M, Kanari P, Partassides D, Loizou E (1998) Study of the British Pharmacopeia method on methimazole (thiamazole) content in carbimazole tablets. J Pharm Biomed Anal 16(5): 785-792.

4. Methimazole oral. In RelayClinical Education [Online] RelayHealth, Ed. Health Reference Center Academic: 2012.

5. Anderson JW (1968) Extraction of enzymes and subcellular organelles from plant tissues. Phytochemistry 7(11): 1973-1988.

6. Palmer JK, Roberts JB (1967) Inhibition of Banana Polyphenoloxidase by 2-Mercaptobenzothiazole. Science 157(3785): 200-201.

7. Pierpoint WS (1966) The enzymic oxidation of chlorogenic acid and some reactions of the quinone produced. Biochem J 98(2): 567-580.

8. Gupta MN, Vithayathil PJ (1982) Isolation and characterization of a methionine adduct of DOPA o-quinone. Bioorg Chem 11(2): 101-107.

9. Aslanoglu M, Peker N (2003) Potentiometric and voltammetric determination of methimazole. J Pharm Biomed Anal 33(5): 1143-1147.

10. Moretti G, Betto P, Cammarata P, Fracassi F, Giambenedetti M, et al. (1993) Determination of thyreostatic residues in cattle plasma by high-performance liquid chromatography with ultraviolet detection. J Chromatogra B: Biomed Sci Appli 616(2): 291-296.

11. Sanchezpedreno C, Albero MI, Garcia MS, Rodenas V (1995) Flow-injection spectrophotometric determination of carbimazole and methimazole. Anal Chim Acta 308(1-3): 457-461.

12. Garcia MS, Albero MI, Sanchezpedreno C, Tobal L (1995) Kinetic determination of carbimazole, methimazole and propylthiouracil in pharmaceuticals, animal feed and animal livers. Analyst 120(1): 129-133.

13. Elbardicy MG, Elsaharty YS, Tawakkol MS (1991) Determination of Carbimazole and Methimazole by First and Third Derivative Spectrophotometry. Spectro Lett 24(9): 1079-1095.

14. Wang A, Zhang L, Zhang S, Fang Y (2000) Determination of thiols following their separation by CZE with amperometric detection at a carbon electrode. J Pharm Biomed Anal 23(2-3): 429-436.

15. Economou A, Tzanavaras PD, Notou M, Themelis D (2004) Determination of methimazole and carbimazole by flow-injection with chemiluminescence detection based on the inhibition of the Cu(II)-catalysed luminol–hydrogen peroxide reaction. Anal Chim Acta 505(1): 129-133.

16. Inoune T, Kirchhoff JR (2000) Electrochemical Detection of Thiols with a Coenzyme Pyrroloquinoline Quinone Modified Electrode. Anal Chem 72(23): 5755-5760.

17. Torriero AAJ, Piola HD, Martinez NA, Panini NV, Raba J, et al. (2007) Enzymatic oxidation of tert-butylcatechol in the presence of sulfhydryl compounds: Application to the amperometric detection of penicillamine. Talanta 71(3): 1198-1204.

18. Torriero AAJ, Salinas E, Marchevsky EJ, Raba J, Silber JJ (2006) Penicillamine determination using a tyrosinase micro-rotating biosensor. Anal Chim Acta 580(2): 136-142.

19. Ruiz Diaz JJ, Torriero AAJ, Salinas E, Marchevsky EJ, Sanz MI, et al. (2006) Enzymatic rotating biosensor for cysteine and glutathione determination in a FIA system. Talanta 68(4): 1343-1352.

20. Molero L, Faundez M, Valle MAd, Río Rd, Armijo F (2013) Electrochemistry of methimazole on fluorine-doped tin oxide electrodes and its square-wave voltammetric determination in pharmaceutical formulations. Electrochimi Acta 88: 871-876.

21. Martinez NA, Messina GA, Bertolino FA, Salinas E, Raba J (2008) Screen-printed enzymatic biosensor modified with carbon nanotube for the methimazole determination in pharmaceuticals formulation. Sens Actuat B Chem 133(1): 256-262.

22. Dorraji PS, Jalal F (2015) Sensitive amperometric determination of methimazole based on the electrocatalytic effect of rutin/multi-walled carbon nanotube film. Bioelectrochem 101: 66-74.

23. Jalali F, Miri L, Roushani M (2013) Electrocatalytic determination of anti-hyperthyroid drug, methimazole, using a modified carbon-paste electrode. Afric J Pharm Pharmaco 7(6): 269-274.

24. Pan M, Fang G, Duan Z, Kong L, Wang S (2012) Electrochemical sensor using methimazole imprinted polymer sensitized with MWCNTs and Salen-Co (III) as recognition element. Biosens and Bioelectron 31(1): 11-16.

25. Shahrokhian S, Souri A, Khajehsharifi H (2004) Electrocatalytic oxidation of penicillamine at a carbon paste electrode modified with cobalt salophen. J Electroanal Chem 565(1): 95-101.

26. Shahrokhian S, Karimi M (2004) Voltammetric studies of a cobalt(II)-4-methylsalophen modified carbon-paste electrode and its application for the simultaneous determination of cysteine and ascorbic acid. Electrochimi Acta 50(1): 77-84.

27. Qi X, Baldwin RP (1996) Selective Oxidation of Thiols to Disulfides at Polymeric Cobalt Phthalocyanine Chemically Modified Electrodes. Journal of the Electrochem Society 143(4): 1283-1287.

28. Wring SA, Hart JP (1992) Chemically modified, carbon-based electrodes and their application as electrochemical sensors for the analysis of biologically important compounds. A review. Analyst 117(8): 1215-1229.

29. Nekrassova O, Lawrence NS, Compton RG (2004) Selective Electroanalytical Assay for Cysteine at a

Boron Doped Diamond Electrode. Electroanalysis 16(16): 1285-1291.

30. Torriero AAJ, Salinas E, Raba J, Silber JJ (2006) Sensitive determination of ciprofloxacin and norfloxacin in biological fluids using an enzymatic rotating biosensor. Biosens Bioelectron 22(1): 109-115.

31. Kashimira C, Tomotake A, Omote Y (1987) Photolysis of the ozonide derived from 1,4-benzodioxins. Synthesis of labile o-benzoquinones. J Org Chem 52(25): 5616-5621.

32. Afkhami A, Nematollahi D, Madrakian T, Khalafi L (2005) Investigation of the electrochemical behavior of some catecholamines in the presence of 4-aminobenzoic acid. Electrochimi Acta 50(28): 5633-5640.

33. Nematollahi D, Tammari E, Sharifi S, Kazemi M (2004) Mechanistic study of the oxidation of catechol in the presence of secondary amines by digital simulation of cyclic voltammograms. Electrochim Acta 49(4): 591-595.

34. Nematollahi D, Rafiee M, Samadi-Maybodi A (2004) Mechanistic study of electrochemical oxidation of 4-tert-butylcatechol: A facile electrochemical method for the synthesis of new trimer of 4-tert-butylcatechol. Electrochimi Acta 49(15): 2495-2502.

35. Torriero AAJ, Shiddiky MJA, Burgar I, Bond AM (2013) Homogeneous electron-transfer reaction between electrochemically generated ferrocenium ions and amine containing compounds. Organometal 32(20): 5731-5739.

36. Rayn MD, Yueh A, Wen-Yu C (1980) The Electrochemical Oxidation of Substituted Catechols. J Electrochem Society 127(7): 1489-1495.